

Electrical Scale-up of Metallurgical Processes

R. Schlanbusch^{*1}, S. A. Halvorsen¹, S. Shinkevich¹ and D. Gómez²

¹Teknova AS, ²Department of Applied Mathematics, University of Santiago de Compostela

*Corresponding author: Teknova AS, Gimlemoen 19, NO-4630 Kristiansand, Norway,
rune.schlanbusch@teknova.no

Abstract: The problem under investigation is electrical scale-up of a generic metallurgical process for primary metal production. In the metal producing step a slag is heated by electric current, typically supplied by an AC three-phase system. The system is described by Maxwell's equations. These equations are analyzed revealing that the properties of the solution is determined by the parameter $(L/\delta)^2$, where L is the linear size of the system and δ is the skin depth. The skin depth is a measure of how deeply the current penetrates a conductor. The effect of changing $(L/\delta)^2$, needs to be considered for scale-up. For cases where $L \lesssim \delta/5$ a DC approximation is appropriate. 2-dimensional AC simulations have been performed. They show unreasonably strong proximity effects, in accordance with theoretical considerations. Such 2D computations should therefore not be applied to get insight for 3D problems. COMSOL simulations are applied to demonstrate the theoretical analysis. Comparison between 2D and 3D simulations clearly shows the strong proximity effect in 2D while it is negligible for the 3D case. Finally, we have applied COMSOL Multiphysics to show how the current distribution for a three-phase system is affected by scale-up. The results agree well with the theoretical prediction. Based on our studies we can conclude that COMSOL Multiphysics is a proper tool for numerical studies of electrical scale-up for metallurgical reactors similar to the ones considered.

Keywords: Scale-up, Maxwell's equations, skin effect, proximity effect, metallurgy

1. Introduction

The last step in many primary metal production processes is to smelt some slag through resistive heating, where the electric current is supplied through carbon electrodes. Designing this kind of processes can be a challenging task due to the complicated nature of the coupling between the different physics at

hand, including thermal, fluid dynamics, chemical reactions and electricity, to name a few. For this reason, the process is typically designed in several steps starting with small scale lab tests, and increase size stepwise, for uncovering and solving the process challenges before building the final production plant; late changes on large facilities obviously can be very costly. The challenges uncovered for the scale-up approach is not only inherited from the design of the process itself, but also appear due to the nature of scaling, such as the L^{n+1}/L^n issue, where L is a length defining the scale. An intuitive example would be to boil a volume of water on the kitchen stove. The container area is proportional to L^2 while the water volume to L^3 . If all linear dimensions are increased by a factor β , the heating area, and hence the heat supply, will be increased by the factor β^2 ; while the water volume will be increased by β^3 . Hence, the time needed to heat the water to the boiling point will be increased by the factor $\beta^3/\beta^2 = \beta$, assuming other factors to be negligible.

Numerous issues like the given example exist with respect to process scale-up. In this paper we study how the well-known skin effect is affecting the process when scale-up is performed. The skin effect is a measure of how deep an alternating current is penetrating a conducting material and can be found by Maxwell's equations [1]. This is a well-studied problem for electrodes, see [2], where the skin effect is studied for a three phase system using three top mounted electrodes. The results obtained through COMSOL also show the "proximity" effect, i.e. the neighboring electrodes influence each other due to the phase change in the induced magnetic fields.

In this paper we study how the skin effect is affecting the process behavior within the furnace by manipulating and non-dimensionalizing Maxwell's equations to obtain a scale-up parameter. Also, we point out a pitfall when using a simplified 2D model for simulation of side mounted electrodes, leading to a drastically increase in the interference of the magnetic field due to neighboring electrodes.

2. Theory

Electric and magnetic fields and their behavior are described by Maxwell's equations

$$\vec{\nabla} \cdot \vec{B} = 0, \quad (1)$$

$$\vec{\nabla} \cdot \vec{E} = \frac{\rho}{\varepsilon}, \quad (2)$$

$$\vec{\nabla} \times \vec{E} + \frac{\partial \vec{B}}{\partial t} = 0, \quad (3)$$

$$\vec{\nabla} \times \vec{B} - \frac{1}{c^2} \frac{\partial \vec{E}}{\partial t} = \mu \vec{J}, \quad (4)$$

where ε is the electric permittivity, μ magnetic permeability, ρ charge density, \vec{B} magnetic field, \vec{E} electric field, c speed of light and \vec{J} is the current density which according to Ohm's law can be expressed as

$$\vec{J} = \sigma \vec{E},$$

where σ is the electrical conductivity. The time derivative of (4) is

$$\vec{\nabla} \times \frac{\partial \vec{B}}{\partial t} = \sigma \mu \frac{\partial \vec{E}}{\partial t} + \frac{1}{c^2} \frac{\partial^2 \vec{E}}{\partial t^2}, \quad (5)$$

where

$$\frac{\partial \vec{J}}{\partial t} = \sigma \frac{\partial \vec{E}}{\partial t} \quad (6)$$

was utilized. Equation (5) can be rewritten as

$$\vec{\nabla} \times (\vec{\nabla} \times \vec{E}) = \sigma \mu \frac{\partial \vec{E}}{\partial t} + \frac{1}{c^2} \frac{\partial^2 \vec{E}}{\partial t^2}. \quad (7)$$

By applying the relation

$$\vec{\nabla} \times (\vec{\nabla} \times \vec{E}) = \vec{\nabla}(\vec{\nabla} \cdot \vec{E}) - \nabla^2 \vec{E} \quad (8)$$

for the electric field, (7) can be written as

$$\nabla^2 \vec{E} = \sigma \mu \frac{\partial \vec{E}}{\partial t} + \frac{1}{c^2} \frac{\partial^2 \vec{E}}{\partial t^2}. \quad (9)$$

In the case of a non-conducting media, $\sigma = 0$, the differential equation reduces to a well-known wave equation

$$\nabla^2 \vec{E} = \frac{1}{c^2} \frac{\partial^2 \vec{E}}{\partial t^2}. \quad (10)$$

By assuming harmonic electric fields, i.e.

$$\vec{E}(\vec{r}, t) = \vec{E}(\vec{r}) \cos(\omega t), \quad (11)$$

the electric field equation (9) can be expressed as

$$\nabla^2 \vec{E} = i\omega \sigma \mu \vec{E} - \frac{\omega^2}{c^2} \vec{E}. \quad (12)$$

The similar result can be obtained for the magnetic field.

For non-dimensionalization and further analysis we define the dimensionless variables

$$\begin{aligned} x &= L\tilde{x}, & y &= L\tilde{y}, & z &= L\tilde{z}, \\ E &= E_0 \tilde{E}, \end{aligned} \quad (13)$$

where L is a characteristic length scale and E_0 is characteristic field strength.

For simplification consider an electromagnetic radiation propagating in the x -direction into an infinite half-plane of conducting media. In this case a linearly polarized electric field has only one non-zero component, $E = E_z(x)$, and (12) can be written as

$$\frac{\partial^2 E}{\partial x^2} - \left(i\omega \sigma \mu - \frac{\omega^2}{c^2} \right) E = 0. \quad (14)$$

By inserting (13) into (14) we obtain

$$\frac{\partial^2 \tilde{E}}{\partial \tilde{x}^2} - 2i \left(\frac{L}{\delta} \right)^2 \tilde{E} + \left(2\pi \frac{L}{\lambda} \right)^2 \tilde{E} = 0, \quad (15)$$

where δ is skin depth, defined as

$$\delta = \sqrt{\frac{2}{\omega \sigma \mu}} \quad (16)$$

and λ corresponds to the wavelength given by

$$\lambda = \frac{2\pi c}{\omega}. \quad (17)$$

If $(2\pi L/\lambda)^2$ is small, the last term in equation (15) can be neglected, and if $(L/\delta)^2$ is small, then the second term can be dropped. Hence, there will be different regimes for the electric field depending on the scale parameter, L :

- Electromagnetic waves, $\lambda \ll L$
- Alternating current (AC), $\lambda \gg L$
 - High frequency, $\delta < L$
 - Low frequency, $\delta \gtrsim L$
- Direct current (DC), $\delta \gg L$.

For our application, $\lambda \gg L$, and electromagnetic waves can safely be neglected. Also observe that the dependency on L/δ is quadratic in the non-dimensional equation (15). Hence, $(L/\delta)^2$ is the appropriate scale-up parameter to be considered. Further, the DC approximation is reasonable if $L \lesssim \delta/5$ since the numerical factor in equation (15), $2(L/\delta)^2$, is less than $1/10$.

For alternating current equation (14) can be approximated as

$$\nabla^2 \vec{E} = \frac{2i}{\delta^2} \vec{E}, \quad (18)$$

which yields the solution

$$E(x) = E_0 e^{-\frac{x}{\delta}} e^{-i\frac{x}{\delta}} \quad (19)$$

with current density

$$J(x, t) = J_0 e^{-\frac{x}{\delta}} \cos\left(\omega t - \frac{x}{\delta}\right). \quad (20)$$

For cylindrical coordinates, the AC-approximation of the equation (12), with non-zero component $E = E_r(r)$, can be expressed as

$$\frac{1}{r} \frac{\partial}{\partial r} \left(r \frac{\partial E}{\partial r} \right) - \frac{2i}{\delta^2} E = 0. \quad (21)$$

A non-singular solution of the equation (21) can be expressed in terms of Bessel function of complex argument [3]

$$E_r(r) = C J_0 \left((1-i) \frac{r}{\delta} \right), \quad (22)$$

where $J_0(x)$ is the zero order Bessel function of the first kind and C is a constant of integration which can be found from boundary conditions. The current density in a cylindrical conductor of radius R has the following spatial distribution

$$J(r) = J_0 \left| \frac{J_0 \left((1-i) \frac{r}{\delta} \right)}{J_0 \left((1-i) \frac{R}{\delta} \right)} \right|. \quad (23)$$

The current distribution (23) for different values of the parameter R/δ is shown in Figure 1. In the case of relatively small skin depth, $\delta \ll R$, using asymptotic expansion of Bessel function for large argument, the current density becomes

$$J(r) \approx J_0 e^{-(R-r)/\delta}, \quad (24)$$

that corresponds to the result (20) of the planar geometry. For example for practical purposes, a ratio $R/\delta \geq 5$ typically indicates less than 6% error will be present when assuming this planar approximation of exponential decay.

The analysis for the full vector equation (9) is more complex. For the isotropic case it gives the same results, i.e. the same scaling parameters $(L/\delta)^2$ and $(L/\lambda)^2$ and hence the same criteria for when the various regimes occur.

Performing analysis for the magnetic field, the non-dimensionalization gives a similar equation with the same scaling results.

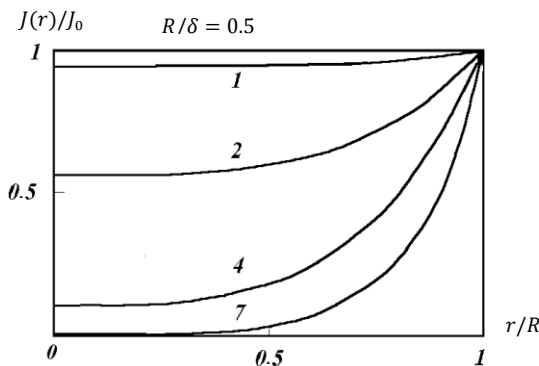


Figure 1. Current distribution in a cylindrical conductor for different values of R/δ .

3. Use of COMSOL Multiphysics

To investigate the theory presented in Section 2 we have developed three different COMSOL models: A 2D with two pairs of one-phase controlled electrodes, a 3D model for the same system and a three-phase 3D model. The 2D model is intended to give an overview of how the current is flowing inside the slag, and to point out a technical challenge by utilizing a 2D model for studying side mounted electrode systems. The challenge lies in the fact that the electrodes are treated as infinite plates, increasing the mutual influence between the magnetic fields of neighboring electrodes, independent of relative distance. The 3D model for the same system shows vital differences between the 2D and 3D cases. The three-phase 3D model is employed to show how the current density inside the slag is affected by scale-up.

The geometry utilized in this study is depicted in Figure 2 with a cylindrical tank containing slag, metal and gas phase. The three cylindrical electrodes are horizontally equiangular in black, see Figure 3. The geometry was parameterized to easily investigate different dimensions of the geometry.

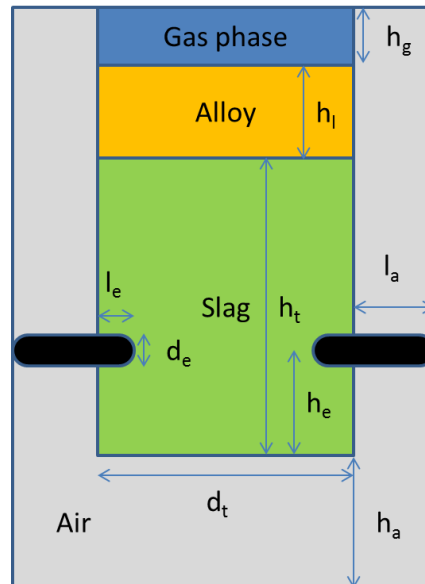


Figure 2. Schematic plot of process geometry.

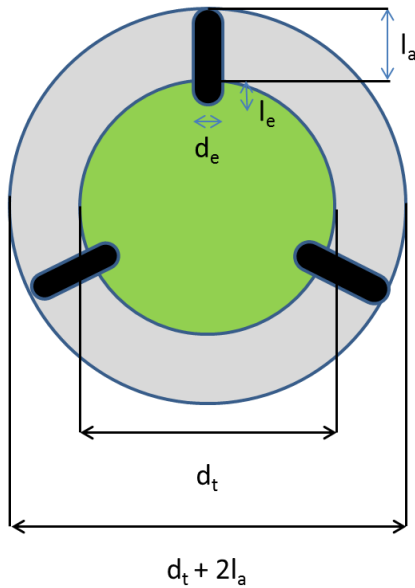


Figure 3. Top view of process geometry.

The physics were modeled by utilizing the time harmonic A-V formulated eddy current model (Magnetic and Electric Fields/Ampère's Law and Current Conservation), while thermal, chemical, mechanical, fluid flow etc. issues were considered out of scope for this work. The model was implemented by removing the two top layers in Figure 2 (metal and gas phase). Moreover, the tank was assumed to be enveloped by an artificial cylinder of electrically insulating material while surrounding space was transparent for the magnetic field, in order to perform suitable FEM numerical computations.

The boundary conditions for the model were as follows: all outward boundaries were considered as magnetically insulated, $\vec{A} \times \vec{n} = 0$; the outward boundaries of the air were considered as electrically insulated, $\vec{j} \cdot \vec{n} = 0$; the top boundary layer of the slag column was assumed to be a perfect conductor, i.e. with zero electric potential, $V = 0$; the outward surface of the electrodes were assumed to have normal current density homogenously distributed over the cross section of the electrodes, $-\vec{n} \cdot \vec{j} = J_i$. The boundary condition for the top of the slag column is a reasonable approximation as most metals have much higher conductivity in liquid metal phase compared with the respective slag. In the three-phase model the current for the electrodes was implemented with a phase shift of

120 degrees between each electrode. In the simulation of metal production we have assumed graphite electrodes. The model parameters are summarized in Table 1 and material properties in Table 2 which give the following values of skin depth and wave length at 50 Hz

$$\begin{aligned} \delta_{\text{Graphite}} &= 14.5 \text{ cm}, \\ \delta_{\text{slag}} &= 2.69 \text{ m}, \\ \lambda &= 6 \times 10^6 \text{ m}. \end{aligned} \quad (25)$$

The geometry for the 2D case is a horizontal plane cutting through the center of four electrodes, see Figure 4, solved utilizing three-component magnetic vector potential with full background field and gauge fixing for A-field. Note that in this simplified model, the electrodes are considered as infinite long plates stretching outward from the model plane. It follows from Ampère's law that the magnetic field due to an infinite current sheet is proportional to the current and independent on distance from the plate. Therefore, the magnetic field inside an electrode depends on the current (and phase) in the neighboring electrodes, but does not depend on the distance between them. Thus, the influence of AC in one electrode on the current distribution in another one becomes significant. This phenomenon is mutual "proximity" effect which can be explained and described by Lenz's law. One can expect that the current density distribution inside an electrode will vary along the thickness direction with one dense side and proportionally non-dense at the other.

The magnetic field between the electrode sheets with currents in the same direction vanishes due to superposition principle of their magnetic fields.

Table 1. Model parameters.

Parameter	Description	Value
d_t	Tank diameter	1.2 m
h_t	Tank height	1.4 m
h_e	Electrode from bottom	0.5 m
d_e	Electrode diameter	0.2 m
l_e	Electrode length in tank	0.15 m
l_a	Electrode length in air	1 m
h_a	Air height below tank	1 m
f	Current frequency	50 Hz
J	Electrode current	14 kA

Table 2. Material properties.

Material	Rel. perm.	Conductivity (S/m)
Graphite	1	$24 \cdot 10^4$
Slag	1	700
Air	1	$1 \cdot 10^{-5}$

4. Simulations

In this section we present simulation results obtained using the models described in Section 3, to verify the results of the theoretical study performed in Section 2. First we present results from studying the phenomena of neighboring electrodes using the 2D model. Two separate electrode pairs (one pair of electrodes is oppositely placed in the furnace) are utilized, and the two pairs are separated by an angle of 60 degrees. Both pairs were supplied with the same AC at zero phase angle through the end of the two top-leftmost electrodes, and grounded at the end of the opposite electrodes (bottom-right). Also gauge fixing for vector A-field was needed. The parameters and material properties given in Table 1 and Table 2 were utilized except for the height.

A plot of the current density norm with directional arrows is shown in Figure 4. It can be seen that the current density inside the electrodes is not uniformly distributed at the ends submerged in the slag nor axis-symmetric along the center of the electrode in air; the latter would be expected if the skin effect was dominating. Instead, the combined proximity effect is observed that was discussed in Section 3. In Figure 5 the magnetic field is plotted from the same simulation showing that in-between the neighboring electrodes the magnetic field is zero, and constant outside the conducting media. There is also a phase shift of 180° between the magnetic fields on the different sides of the neighboring electrode pairs.

Inside an electrode the field will be determined by the boundary conditions on each side, with some minor corrections at each electrode end. The problem is equivalent to considering half part of a conducting sheet that is twice as thick. Here, the magnetic field will be zero at the center due to symmetry. Hence, it follows that the fields within each of the electrode pairs will be independent of the

distance and the angle between them (except close to the electrode ends). To show this effect we made an additional 2D COMSOL model where each electrode pair was replaced by one electrode being twice as thick. Figure 6 shows the current distribution across an electrode for the original model, while Figure 7 shows the result for the latter case. Clearly, the current distribution in Figure 6 corresponds to half of the curve in Figure 7.

For a similar 3D model, with two pairs of one-phase controlled electrodes and the parameters given in Table 1 and Table 2, the magnetic field distribution is shown in Figure 8. We can see that the induced magnetic field decays relatively fast outside the electrodes in contrast to the case of the 2D model shown in Figure 5. Therefore the mutual proximity effect is negligible and the current density is not affected by neighboring electrodes in the 3D case, see Figure 9.

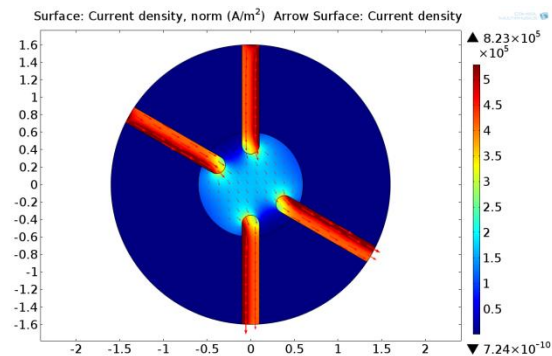


Figure 4. Current density distribution for 2D model with two pairs of one-phase controlled electrodes.

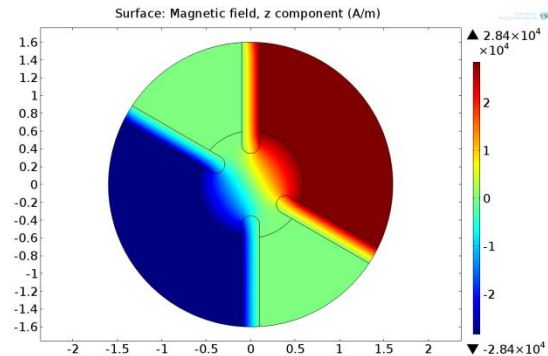


Figure 5. Magnetic field distribution for 2D model with two pairs of one-phase controlled electrodes.

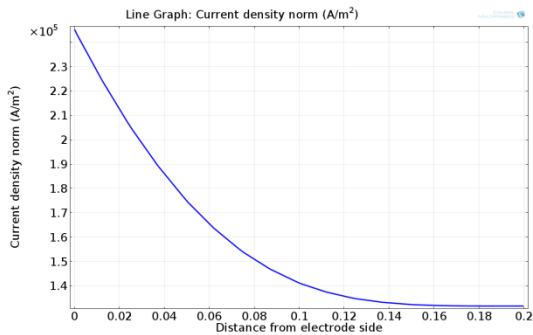


Figure 6. Current density across an electrode for 2D model with two pairs of electrodes.

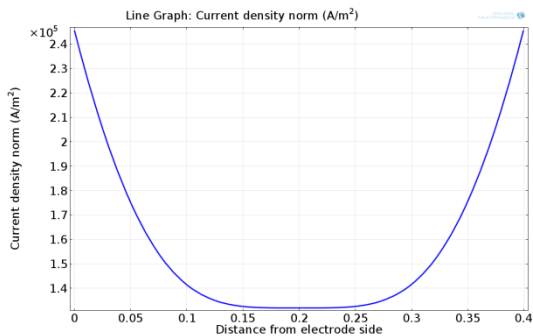


Figure 7. Current density across an electrode with twice thickness for 2D model with two electrodes.

We have also performed some 2D three-phase simulations for a 2D geometry corresponding to the 3D model in Figure 10. The simulations showed very strong proximity effect also in this case. Based on our analyses and the simulations we will discourage the use of 2D AC models to get insight relevant for 3D cases.

The proximity effect is caused by the coupling between alternating electric and magnetic fields. We can therefore not preclude use of DC models provided such approximation is relevant. The COMSOL model for Electric Currents (ec) might be relevant.

In the next simulation, the full 3D model with three-phase controlled electrodes was utilized and based on the physical parameters and material properties given in Table 1 and 2. The current density distribution is shown in Figure 10.

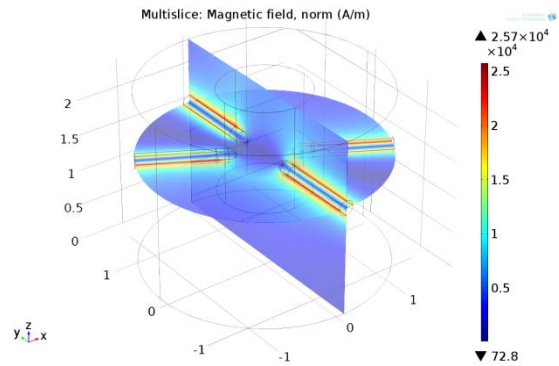


Figure 8. Magnetic field distribution for 3D model with two pairs of one-phase controlled electrodes.

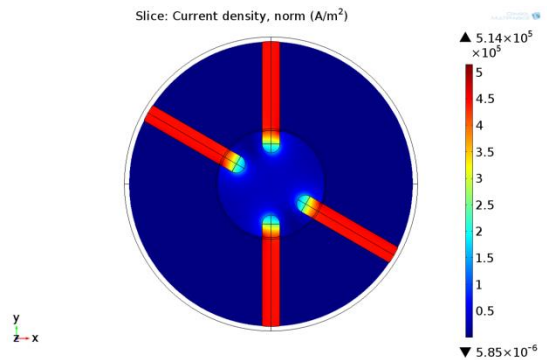


Figure 9. Current density distribution for 3D one-phase current model.

To verify our theoretical findings we consider the dimensionless scaling parameter $(L/\delta)^2$, which in the case of cylindrical conductor of radius R naturally becomes $(R/\delta)^2$, where the skin depth δ depends only on material properties and current frequency. The current density as a function of distance from electrode center for the original geometry is shown in Figure 11 and Figure 12 respectively. It can be seen that the skin effect is not significant and the current is almost uniform when the skin depth is bigger than the radius of the electrode (the dimensionless parameter $(R/\delta)^2 \approx 0.5$), while after tripling electrode radius, $(R/\delta)^2 \approx 4$, the current density at the center of an electrode is reduced to 54% of its value on the boundary and the skin effect plays an important role for the current distribution. These results of simulation are in a good agreement with the theoretical prediction (22) shown in Figure 1.

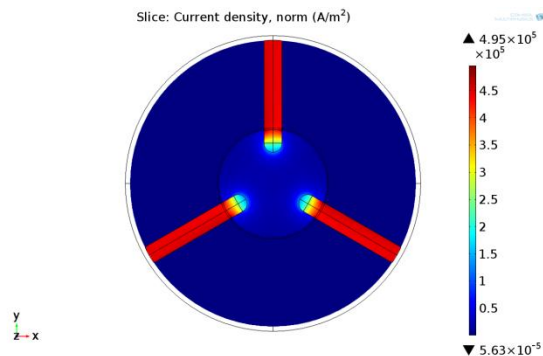


Figure 10. Current density distribution for 3D model with three-phase controlled electrodes.

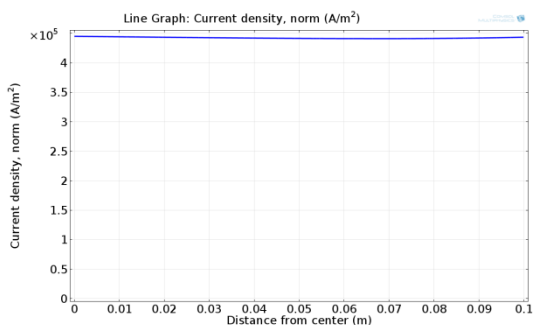


Figure 11. Current density across an electrode for standard geometry.

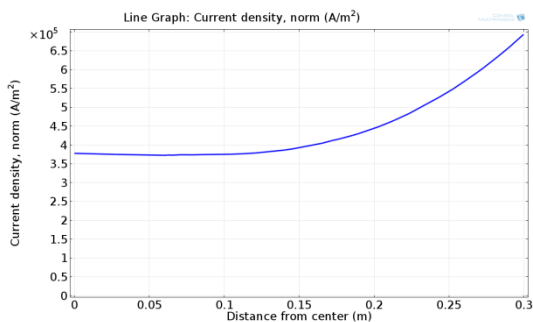


Figure 12. Current density across an electrode for tripled all linear dimensions.

5. Conclusions

Based on analysis of Maxwell's equations we have shown that there are three different regimes for the solution, depending on the electromagnetic frequency and the size of the system to be analyzed:

- Electromagnetic waves
- Alternating current (AC)
- Direct current (DC)

The regime for electromagnetic waves is not relevant for primary metal production.

For electrical scale-up, where the physical system is enlarged by the same factor in all directions, the properties are determined by the parameter $(L/\delta)^2$, where L is the linear size of the system and δ is skin depth.

The DC approximation is reasonable if $L \lesssim \delta/5$.

2-dimensional AC simulation results show unreasonably strong proximity effects and should not be applied to get insight relevant for 3D problems.

COMSOL simulation results agree well with our theoretical analysis. COMSOL Multiphysics is therefore a proper tool for numerical studies of electrical scale-up for metallurgical reactors similar to the ones studied in this article.

6. References

1. J. C. Maxwell, A dynamical theory of the electromagnetic field, *Philosophical Transactions of the Royal Society of London*, **Vol. 155**, pp. 459-512 (1865)
2. H. L. Larsen, Current Distribution in Electrodes of Industrial Three-phase Electric Smelting Furnaces, In: *Proceedings of the 2006 Nordic COMSOL Conference* (2006)
3. D. Voltmer, Fundamentals of Electromagnetics: Quasistatics and Waves, In: *Synthesis Lectures on Computational Electromagnetics*, **Vol. 2**, Morgan & Claypool (2007)

7. Acknowledgements

The authors would like to thank Regional Research Fund Agder (RFF Agder) for their financial support.